University of Thi -Qar Journal for Engineering Sciences
http://www.doi.org/10.31663/tqujes13.1.437(2023)
Vol.13.1(January2023)

ISSN :2664- 5572 (online)
ISSN:2664-5564 (print)
Available at http://jeng.utq.edu.iq
utjeng@ utq.edu.iq

State Space Modelling and Disturbance Evaluation for Matrix Converter Drives

Alyaa Muhsen Manati [†], and Ali Salam Al-Khayyat [‡]
[†] Department of Electrical and Electronics Engineering, University of Thi-Qar, Al-Nassriyah, Iraq, alyaa-m@utq.edu.iq.
[‡] Department of Electrical and Electronics Engineering, University of Thi-Qar, Al-Nassriyah, Iraq, ali-al-khayyat@utq.edu.iq..

Abstract

The Matrix converter technology draws significant interest in motor drive applications. This is due to the advantages it can offer, like providing high quality input and output currents and compact structure. However, some unsolved problems strict its industrial use, one of these main problems is the stability of operation caused by the voltage distortion and/or the load torque disturbances. Using steady state small signal analysis, the matrix converter drive system driving an induction motor and equipped with an input filter will be presented in this paper, the stability of the system will be examined and the factors that influence it will be defined. A method of investigating the complex system with multiple-inputs multiple-outputs in simple fashion will be presented. Matlab/Simulink computer software is used to obtain simulation results to verify the mathematical model. The analysis will be carried out using transfer function analysis and the migration of eigenvalues on the simulation results. Where it has noticed that the stability is significantly affected by the system parameters, while the damping resistor of the filter affect the system stability directly.

Keywords: Matrix converter; Matrix Converter Drives; Stability Analysis.

1. Introduction

Matrix converters are capable of providing sinusoidal input and output currents, more compact structure, bidirectional power flow and wide range of input power factor control. Thus, matrix converters draw substantial consideration amongst researchers as an alternative for Rectifier/Inverter types of converters mainly because it doesn't have DC link energy storage elements, which are often bulky**.** Modulation techniques and technology overview have been presented and summarized and discussed as well as many control strategies**.** Input filter is an important stage of matrix converters design, as it provides better input current quality and decreases the input voltage distortion. However, using a fast closed loop control as the ones used for controlled rectifiers or direct torque control presents instability in operation**.** Moreover, the absence of the intermediary energy storage passive element, and the presence of the input filter drive the matrix converters to unstable operation **[1]–[3].**

Matrix converters allow wide range of controlling the output power, this is because the phase angle between the space vectors of input voltage and current. This can be used to outline many modulation strategies of input current, and hence improve the input current quality as well as, providing sinusoidal output voltages**.** One of the most basic modulation strategies is constructed on the detection of zero crossing of input voltage, this helps to synchronize the input current phase and generate sinusoidal waveforms. Yet, the presence of voltage disturbances and the fact that there is no perfect supply (i.e. balance sinusoidal and zero impedance) determines low order harmonics in input voltage. Methods of providing feed-forward compensation to calculate the duty cycles for balance voltages have been developed, still, the presence of input filter leads to instability especially when the maximum output power is exceeded. Matrix converter stability has been studied using small-signal and large-signal analysis methods, and it has been found that the system stability and power limits are affected by the system parameters particularly the input filter. Furthermore, digital low pass filter has been developed to reduce the input voltage disturbances and increase the stability limits by providing reference frame. Also, it has been proven that cycle period delay presented by digital control can affect the power limit to some extent. System parameters have significant influence on stability operation, this has been proven using small signal analysis by filtering the magnitude and angle of input voltage space vector**.** Additionally, alongside with system parameters, the power losses in the converter system have been considered in to calculate the stability limits. Thereby, it can be concluded that system parameters, filter and supply impedances and power losses in matrix converters have supreme effect on stability of matrix converters, and it can be the corner stone of designing robust and reliable system **[4]–[8].**

In this paper, stability of matrix converters is a significant dilemma and it has been investigated for different types of applications, like aerospace, pumps, fans and a new motor drive method known as integrated matrix converter induction motor drive, in which the converter is accommodated inside the motor case.

This paper is arranged in six sections; section 2: introduce an overview about matrix converter, which consists of fundamentals of operation and limitations, and then a brief demonstration of modulation techniques is

presented. Section 3: deals with modulation techniques with the aid of Matlab simulations. Section 4: stability theories will be presented, which can be used. Section 5: a dynamic model of the matrix converter system is derived and implemented in Matlab and several analysis techniques are used to evaluate the system in section 6.

2. Matrix Converter

The matrix converter is a potential alternative for other converter topologies due to its many benefits. As seen in Figure 1, it comprises of a configuration of $[n \times m]$ frames, where (n) stands for the input phases source and (m) for the output phases load (i.e. three phase AC source converted to three phase AC load). The output voltage can therefore be created by connecting any output terminal to any input one. Furthermore, unlike the well-known VSI converter (shown in Figure 2), the matrix converter lacks a DC link stage, making it more compact. Typically, the DC link capacitor or inductor takes up roughly 30 to 50 percent of the converter's overall volume. Additionally, a matrix converter may produce sinusoidal input current and output voltage for any desired amplitude and frequency, as well as unity input power factor for any load state (inductive or capacitive), which can be accomplished utilizing certain modulation techniques. Additionally, due to the bidirectional switches, it has the capacity to regenerate current in both ways. [3], [5], [7], [9]–[11].

The matrix converter is subject to a few limitations, though. Since it is often driven by a voltage source, the input phases must never be shorted. Second, because the load is often an inductive load, the output terminals should never be opened (i.e. induction machine). Additionally, harmonics produced by periodically switching the current on and off are frequently linked to matrix converters. These harmonics have an impact on the performance of the load and, more crucially, the quality of the input power. As a result, filters are crucial in the development of high performance. The power density and weight of power converters are also crucial factors. Additionally, while creating input filters for static power converters powered by AC, the following standards should be adhered to:

- Performing the noise attenuation of the switching;
- Minimizing the displacement angle the current and the voltage at the input;
- Ensuring there is stability of the system.

There are more variables related to price, voltage attenuation, system effectiveness, and the modification of the filter parameter. Therefore, matrix converters use passive devices to filter out the harmonics (i.e., lower converter losses), therefore in this scenario, the size, price, and overall converter losses have been compromised **[1], [3], [7]–[9], [12].**

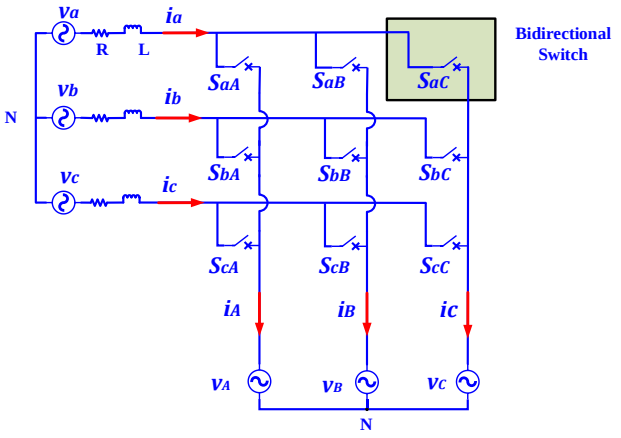

Figure. 1 Simple diagram of the Matrix converter

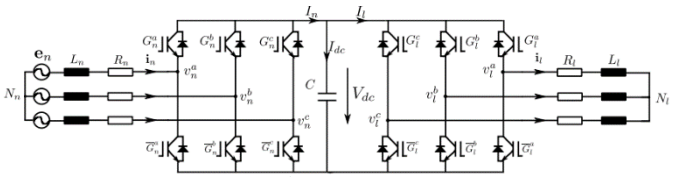

Figure. 2 Diagram of VSI back-to-back converter

The rectifying stage and the inverting stage are typically found in conventional converter topologies' two power conversion stages, however there is just one in the matrix converter. This restricts the topology so that neither the input nor the output terminals may ever be short-circuited or open-circuited. Figure 3's form serves as an illustration of the switching method.

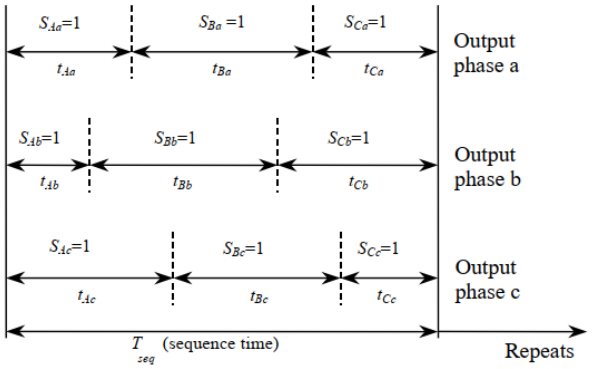

Figure. 3 Switching pattern general form [3]

The relationship between the input and output voltage can be defined as follows:

$$\begin{bmatrix} V_a(t) \\ V_b(t) \\ V_c(t) \end{bmatrix} = \begin{bmatrix} S_{Aa}(t) & S_{Ba}(t) & S_{Ca}(t) \\ S_{Ab}(t) & S_{Bb}(t) & S_{Cb}(t) \\ S_{Ac}(t) & S_{Bc}(t) & S_{Cc}(t) \end{bmatrix} * \begin{bmatrix} V_A(t) \\ V_B(t) \\ V_C(t) \end{bmatrix} \quad (1)$$

where:

$$V_0 = \begin{bmatrix} V_a(t) \\ V_b(t) \\ V_c(t) \end{bmatrix} \text{ and } V_i = \begin{bmatrix} V_A(t) \\ V_B(t) \\ V_C(t) \end{bmatrix}$$

Hence; $[V_o] = [T]\,[V_i]$

The transformation matrix [T] is known as "instantaneous transfer matrix" which can also be used for obtaining input currents in this form:

$$I_i = \begin{bmatrix} i_a(t) \\ i_b(t) \\ i_c(t) \end{bmatrix} \text{ and } I_o = \begin{bmatrix} i_A(t) \\ i_B(t) \\ i_C(t) \end{bmatrix}$$

$$[I_i] = [T]^T [I_o]$$

Where: $[T]^T$ is the transposed instantaneous transfer matrix.

The output voltage can be created with any desired magnitude and switching frequency by changing the duty-cycle of the bidirectional semiconductor switches at a high switching frequency. The instantaneous transfer matrix can be used to describe the duty cycle of each bidirectional switch as follows:

$$M(t) = \begin{bmatrix} m_{Aa}(t) & m_{Ba}(t) & m_{Ca}(t) \\ m_{Ab}(t) & m_{Bb}(t) & m_{Cb}(t) \\ m_{Ac}(t) & m_{Bc}(t) & m_{Cc}(t) \end{bmatrix} \quad (2)$$

Where: $m_{kj}(t) = t_{kj}/T_{seq}$

$$0 < m_{kj} < 1 \; k = \{A, B, C\} \; j = \{a, b, c\}$$

Hence: $V_o(t) = M(t)\, V_i(t)$ and $I_i(t) = M(t)^T\, I_o(t)$

Figure 4 illustrates the output voltage (a) and current (b) waveforms of a matrix converter [4], [5], [7], [9]–[11], [13]–[17].

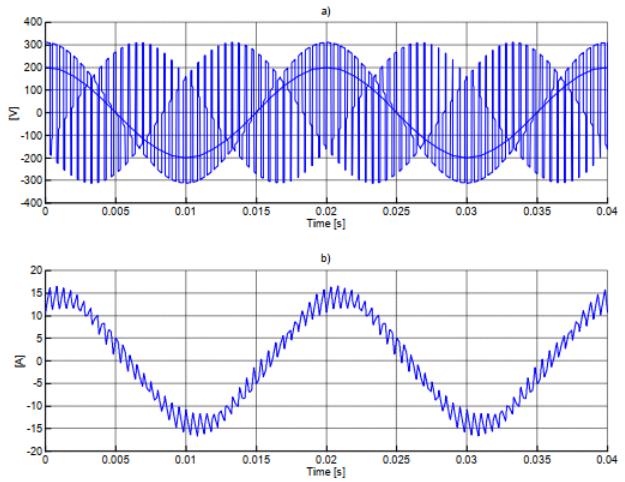

Figure. 4 Output voltage and input current waveforms of matrix converter

3.Modulation Techniques

Output voltages and input currents of a matrix converter can be represented as:

$$v_i = V_{im} \begin{bmatrix} \cos(\omega_i t) \\ \cos(\omega_i t + 2\pi/3) \\ \cos(\omega_i t + 4\pi/3) \end{bmatrix} \quad (3)$$

$$I_o = I_{om} \begin{bmatrix} \cos(\omega_o t + \emptyset_o) \\ \cos(\omega_o t + \emptyset_o + 2\pi/3) \\ \cos(\omega_o t + \emptyset_o + 4\pi/3) \end{bmatrix} \quad (4)$$

Then the modulation matrix can be found as:

$$V_o = qV_{im} \begin{bmatrix} \cos(\omega_o t) \\ \cos(\omega_o t + 2\pi/3) \\ \cos(\omega_o t + 4\pi/3) \end{bmatrix} \quad (5)$$

$$I_i = q\cos(\emptyset_o)\, I_{om} \begin{bmatrix} \cos(\omega_i t + \emptyset_i) \\ \cos(\omega_i t + \emptyset_i + 2\pi/3) \\ \cos(\omega_i t + \emptyset_i + 4\pi/3) \end{bmatrix} \quad (6)$$

Where: $S_{Aj} + S_{Bj} + S_{Cj} = 1 \; j = \{a, b, c\}$

And q: is the gain between input and output voltages.

Hence the basic solutions are:

$M_1 =$

$$\frac{1}{3}\begin{bmatrix} 1+2q\cos(\omega_m t) & 1+2q\cos(\omega_m t - 2\pi/3) & 1+2q\cos(\omega_m t - 4\pi/3) \\ 1+2q\cos(\omega_m t - 4\pi/3) & 1+2q\cos(\omega_m t) & 1+2q\cos(\omega_m t - 2\pi/3) \\ 1+2q\cos(\omega_m t - 2\pi/3) & 1+2q\cos(\omega_m t - 4\pi/3) & 1+2q\cos(\omega_m t) \end{bmatrix} \quad (7)$$

Where $\omega m = (\omega o - \omega i)$ which gives same displacement angle between input and output (i.e. $\Phi i = \Phi o$).

$M_2 =$

$$\frac{1}{3}\begin{bmatrix} 1+2q\cos(\omega_m t) & 1+2q\cos(\omega_m t - 2\pi/3) & 1+2q\cos(\omega_m t - 4\pi/3) \\ 1+2q\cos(\omega_m t - 2\pi/3) & 1+2q\cos(\omega_m t - 4\pi/3) & 1+2q\cos(\omega_m t) \\ 1+2q\cos(\omega_m t - 4\pi/3) & 1+2q\cos(\omega_m t) & 1+2q\cos(\omega_m t - 2\pi/3) \end{bmatrix} \quad (8)$$

Where $\omega m = (\omega o + \omega i)$ which gives reverse phase displacement angle between input and output (i.e. $\Phi i = -\Phi o$), combining the two equation yields the input displacement factor control [6], [7], [9], [16], [18]-[23], [24]-[27].

This results in the direct transfer function technique, which is valid in the sense that the output voltage corresponds to the demand voltage. However, in order for this to work, the demand voltage must always fit inside the input voltage envelope (Tseq). As seen in Figure 5, this denotes the highest output voltage that may be synthesised, which in this instance is 50%. The output voltage ratio can be expanded by dispersing the null output switching states (i.e., those that link the output terminals to the same input terminal), as shown in Figure 6. Therefore, increasing the voltage ratio by adding the common-mode voltage to the demand voltage results in a higher voltage ratio of $(\sqrt{3}/2 = 87\%)$, as shown in the following equation:

$$V_o = qV_{im} \begin{bmatrix} \cos(\omega_o t) - \frac{1}{6}\cos(3\omega_o t) + \frac{1}{2\sqrt{3}}\cos(3\omega_i t) \\ \cos(\omega_o t + 2\pi/3) - \frac{1}{6}\cos(3\omega_o t) + \frac{1}{2\sqrt{3}}\cos(3\omega_i t) \\ \cos(\omega_o t + 4\pi/3) - \frac{1}{6}\cos(3\omega_o t) + \frac{1}{2\sqrt{3}}\cos(3\omega_i t) \end{bmatrix} \quad (9)$$

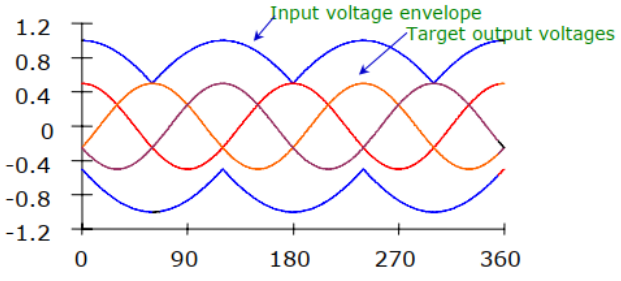

Figure. 5 Maximum voltage achieved of 50%

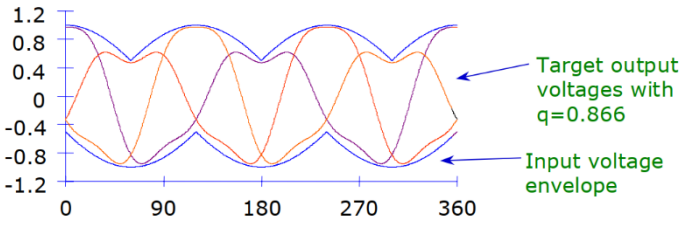

Figure .6 Maximum voltage achieved of 87%

3.1. Venturini Modulation Method

The first approach of Venturini is defined by using the duty cycle matrix approach, as presented in equations (7) and (8), which can be arranged as:

$$m_{Kj} = \frac{t_{Kj}}{T_{seq}} = \frac{1}{3}\left[1 + \frac{2v_K v_j}{V_{im}^2}\right] \quad (9)$$

Where $K = A, B, C$ and $j = a, b, c$.

Though the target voltage will never be greater than 50% of the input voltage due to the impossibility of effectively applying these formulae. As a result, the Venturini optimal method is applied, which uses the common-mode approach to boost the output voltage ratio to 87%. However, a real-time model cannot actually use this approach, hence it can be expressed as follows instead:

$$m_{Kj} = \frac{1}{3}\left[1 + \frac{2v_K v_j}{V_{im}^2} + \frac{4q}{3\sqrt{3}}\sin(\omega_i t + \beta_K) * \sin(3\omega_i t)\right] \quad (10)$$

Where $K = A, B, C$, $\beta_K = 0, {}^{2\pi}/_{3}, {}^{4\pi}/_{3}$ and $j = a, b, c$

Additionally, modern processors are capable of deriving this method voluntarily, and the input displacement factor control can be demonstrated. However, it will come at the expense of the maximum synthesised output voltage [4], [6], [7], [10], [12], [14]-[16], [18], [27]-[29].

3.2 Scalar Modulation Method

The scalar modulation approach [11] on the direct calculation of the switching signals on instant measurements of the input voltage. The following formulae compare the magnitude of the input voltages with the instant measurement:

$$m_{Lj} = \left[\frac{(v_j - v_M) * V_L}{1.5V_i * m^2}\right] \quad (11)$$

$$m_{Kj} = \left[\frac{(v_j - v_M) * V_K}{1.5V_i * m^2}\right] \quad (12)$$

$$m_{Mj} = 1 - (m_{Lj} + m_{Kj}) \quad (13)$$

Where $j = a, b, c$

Additionally, by combining the common-mode (i.e., adding the third harmonic) with the demand voltage, a voltage ratio of up to 87% can be achieved. The switching timing is the same as Venturini's method, despite significant changes. The maximum output voltage ratio (q) in the scalar approach is fixed at $(\sqrt{3}/2 = 87\%)$, which is the fundamental distinction between it and the Venturini approach. As a result, the output voltage quality is unaffected by this approach; nevertheless, when the Venturini's approach is better, worse voltage quality may be observed at low switching frequencies. The duty cycle and modulation are expressed as:

$$m_{Kj} = \frac{1}{3}\left[1 + \frac{2v_K v_j}{V_{im}^2} + \frac{2}{3}\sin(\omega_i t + \beta_K) * \sin(3\omega_i t)\right] \quad (14)$$

3.3 Optimum Venturini Modulation Method

In this method the third harmonic of the input and output voltage frequency is added to obtain the modulation matrix. Additionally, the voltage transfer ratio of this method is 86.6%. The voltage equations are given as:

$$[V_o(t)] = \begin{bmatrix} V_a(t) \\ V_b(t) \\ V_c(t) \end{bmatrix}$$

$$[V_o(t)] = q * V_{im} * \begin{bmatrix} \cos(\omega_o t) - \frac{1}{6}\cos(3\omega_o t) + \frac{1}{2\sqrt{3}}\cos(3\omega_i t) \\ \cos(\omega_o t + {}^{2\pi}/_{3}) - \frac{1}{6}\cos(3\omega_o t) + \frac{1}{2\sqrt{3}}\cos(3\omega_i t) \\ \cos(\omega_o t + {}^{4\pi}/_{3}) - \frac{1}{6}\cos(3\omega_o t) + \frac{1}{2\sqrt{3}}\cos(3\omega_i t) \end{bmatrix} \quad (15)$$

Assuming a unity displacement power factor, the modulation matrix can be derived from the following equation:

$$m_{Kj} = \frac{1}{3}\left[\frac{1}{3} + \frac{2v_K v_j}{3V_{im}^2} + \frac{4q}{9\sqrt{3}} * \sin(\omega_i t + \beta_K) * \sin(3\omega_i t)\right] \quad (16)$$

For $K = A, B, C$ and $j = a, b, c$ and β_K=0, -2π/3, 2π/3.

4. Stability of Matrix Converter

Matrix converters have superior advantages over other converters used as drives, particularly in that they have no bulky energy storage devices (and hence have a smaller size) and they have better input power quality in terms of displacement power factor, which provides sinusoidal waveforms of input currents and output voltages and unity input displacement factor. However, like any other type of converters the switching action in matrix converters tends to distort the input current with harmonics, and hence distort network voltages and affect other systems**.** Therefore, it is necessary to equip the converter with an input filter providing compliance of design standards to limit the electromagnetic interference and dampen the sudden transient voltages from the supply, which protects not only the converter but also the load, so it improves the whole system's reliability [4], [6], [7], [14]–[16], [29]–[31].

Filters can affect system stability. The stable system can become unstable due to the type of the converter or the applied control method. This problem becomes crucial when the control design has a very fast closed-loop response, so any disturbance caused by the input voltage or the motor system itself drives the system to be unstable (i.e. driving the output power beyond acceptable levels). This problem begins with small voltage distortion, which is then used to calculate the demanded duty cycle of the converter (undertaken by the controller) and the amplitude of the distorted signal becomes more viable, which eventually leads to unstable operation [16], [21], [28].

In nonlinear system such as the matrix converters, the solution transient of the frequency domain analysis cannot be simulated, as it does not have information on how the steady state system behaves to perturbations. Therefore, frequency domain techniques are not adequate for testing stability of such systems, thus a complementary technique of stability analysis needs to be used. The most common stability analysis types used for examine the stability of such system are small-signal analysis and large-signal analysis. In small signal regime the equations of the system need to be linearized about an operating point, then the effect of small signal perturbations needs to be neglected. However, for large signal regime the equations of the system are linearized about large-signal periodic regime; both have different purposes and lead to different stability analysis.

4.1 Small-Signal Analysis

If the system encloses in one or more small-signal independent sources of which the solution is linear regarding these input sources then it can be analyzed. Similar to the DC solution the small signal regime has the same stability properties, which are acquired by setting every input source to zero value. This can be derived due to the simple fact that the system is linear to these sources. Moreover, the superposition approach can fulfill these requirements, so the stability analysis will be identical to the DC solutions. By suppressing the time varying input sources, the small signal stability analysis can be done. The system response due to any disturbance of any frequency can be analyzed by linearizing it about an operating point (i.e. DC solution). Hence, if small signal stability can be defined as being when the system oscillates by means of a small disturbance that can be damped, such that the state variables of the system do not deviate much for small time, the system is defined as stable. This can be affected by many aspects such as initial conditions, control devices used and the system itself.

From this, any system cannot function practically if it is unstable in terms of small signal analysis; in other words, any system needs to be examined by small signal analysis under definite functioning conditions. However, this method has slow computational speed, and deeper examination of the physical cause of system instability cannot be undertaken, which is considered as its main weakness. The Lyapunov linearized method offers a beneficial tool for small signal analysis, which is based on the productive outcomes of Eigen solution analysis, which have been extensively used in small signal analysis.

Maximum voltage transfer ration of a matrix converter model using small signal analysis was developed in, facilitating the calculation of maximum voltage ratio and the cut-off frequency of the input filter for stable operation. This was proved through simulation and experimental results **[7], [14], [16], [32].**

In small signal analysis was performed using the migration of eigenvalues of a linearized state matrix of different designs of input filter and non-ideal power supply, and the instability occurrence was checked. Moreover, the maximum power limit of the converter as function of input filter and power supply parameters was developed, which simplified the design procedure of input filter.

Another small signal model was examined for two different types of load: passive R-L load and an induction motor. The model was used to study the stability of the system using the eigenvalue locus, which then proved to be affected by the system parameters, like source impedance, filter elements and filter time constant. However, the experimental results showed a significant difference compared with small signal model, which is due to the discrete components and digital control.

4.2 Large-Signal Analysis

The ability of a certain system to move from one steady state operating point caused by a certain disturbance to another is defined as large signal stability. It includes major disturbances like faults, switching failures, sudden load change etc. so its main objective is to examine if the system will return to steady state condition or not. In a large signal model based on physical observation of matrix converter was examined, and by approximating the system performance using this approach the stability of the system was determined, and the nonlinear reasons behind the instability phenomena appreciated. The instability regions and the physical reasons behind them were identified, and the method is useful for certain estimations for adequate components used for better design [19], [24], [27].

4.3 State Space Analysis

A unified methodology of treating wide range of problems in time domain analysis is provided using state space modelling. This method assumes that development over time for a certain system can be determined using series of unobserved vectors, which are related with a series of observations; this relationship is known as state space model. The quantities representing the state are known as state variables, and the theoretical space spanned by those variables is known as state space. For instance, for a moving car, the speed of the car and the position of other cars on the road can be presented as state variables, yet the selection of the state variables is not unique, so for the last example the states could be the velocity of other cars relating them to the car or their positions on the road etc. It is worth noting that when choosing different state variables, the set of dynamic equations will be different for the same system. However, the solution will yield the exact same essential characteristics of that system in terms of stability, performance and robustness.

The freedom of selecting the state variables increases the flexibility of this approach, but provided that the minimum number of state variables should be selected to describe a certain system. This is to say, state variables should not be too many or too few, but rather it is common to choose (n) state variables, where (n) represents the order of the system. This approach is handy if the system order is determined from its differential equations, as it is easy to identify the order of these equations. However,

determining the order from system transfer function could have errors, because the poles and zeros of a certain transfer function might be similar, and hence cancel each other. This error could identify an unstable system as stable, and vice-versa. This problem can be evaded by simply obtaining the state variables from system differential equations. Furthermore, another issue that should be considered is that the state variables should not be linearly dependent in the same state space representation. Additionally, in contrast to classical control approaches, this approach works directly from dynamic system differential equations in time domain. This is done by representing the high order differential equations by sets of first order equation, which make it possible to solve them in time domain. Furthermore, since the system can be characterized by first order number of inputs and outputs, this method does not distinguish between SISO systems and MIMO systems, providing more efficient design and analysis. For nonlinear systems, state space representation offers direct design and analysis, by linearizing about an operation point, which is a totally impossible using classical control method. This property allows using linear algebraic manipulations to the system, which can be easily programmed and analyzed on computers.

State space linear equation consists of two equations; the state equation and the output equation, as shown below:

$$\dot{X}(t) = Ax(t) + Bu(t) \quad (17)$$

$$y(t) = Cx(t) + Du(t) \quad (18)$$

Where (A, B, C, D) are the coefficient matrices provided that the row dimensions should equal the order of the system, hence the dimensions of matrices (A, B, C, D) should be as $(n \times n), (n \times r), (p \times n), (p \times r)$ respectively. Where (n) is the number of state variables, (r) is the number of inputs and (p) is the number of outputs [**4], [6], [7], [14], [15], [29], [30]**.

4.4 Transfer Function Analysis

The overall transfer function is calculated by obtaining the transfer function of each component in the system, then, with the aid of laws and interconnection relations, algebraic equations are produced containing components transfer functions, and these equations can be solved in frequency domain, which is used to calculate certain input in Laplace transform to an output in Laplace transform. This approach is useful to derive transfer functions of single input single output SISO out of Laplace transform of state equations of multiple input multiple output MIMO system. Hence, frequency response or root locus of each single output from each single input can be obtained. To derive the transfer function of a system with n state variable from state space model equations (17, and 18) we have:

$$G(s) = C(sI - A)^{-1}B + D \quad (19)$$

Which is defined as the system transfer function G(s).

Additionally, by calculating the determinate of $(sI - A)$, it can be noted that they are the same as the product of diagonal elements of it, known as the characteristic polynomial of matrix A. The roots of this are known as the eigenvalues of matrix A, defined as the dynamic behaviour of the system such as natural frequency, system type and damping factor. Moreover, a "strictly proper" transfer function results if matrix $D = 0$, as the degree of numerator is less than that of denominator, which is defined as a direct connection between input and output. On the other hand, a "proper" transfer function results if matrix $D \neq 0$, as the numerator and denominator has the same degree.

Hence, if no cancelation between poles and zeros of transfer function takes place, then the poles of the system are the same as the eigenvalues of matrix A.

Matrix converter drive system can be estimated by a State Space linearized model using the input and output system dynamic equations. Then feedback control can be applied to achieve fast response to demand signal with zero steady state error. However, disturbance signals are often presented, either from disturbances in input voltages or from the load itself (i.e. distorted back e.m.f., machine slut harmonics or disturbance from the associated load). These disturbance signals affect the output signals, and if the controllers are not designed properly, the outcome of these signals will drive the system to unstable regions. Traditional control approaches such as PID controllers cannot offer very high accuracy, especially if system like matrix converter drive is considered, thus feedback controls are often implemented to efficiently reduce these disturbances. It is possible to analyze the noise in the output signal by observing the effect of it in the error signal, which is fed to the controller. Therefore, feedback loop gain should be big over a wide range of disturbance frequencies so that it can reach minimal steady state error, and hence, to some extent, reject these noises.

4.5 Eigenvalue Analysis

The characteristic polynomial of the system transfer function mentioned earlier is equal to the denominator polynomial of that system, which is equal to the determinate of $SI - A$, therefore the poles of the transfer function are equal to the roots of characteristic equation. Using linear algebra, eigenvalues for a linear time invariant system can be obtained as:

$$Av_k = \lambda_k v_k \quad (20)$$

Where, λ_k represent the eigenvalues of the matrix A, and v_k represents the associated eigenvector, which can be written as:

$$(\lambda I - A)v = 0 \quad (21)$$

and for $(v \neq 0)$ this must be true:

$$|(\lambda I - A)| = 0 \quad (22)$$

Hence, the poles of the matrix A are the same as the eigenvalues of matrix A, as the characteristic equation roots are the eigenvalues. Furthermore, since the matrix A holds information obtained from the characteristic equation of the system, it can describe the system properties, such as stability and performance, which is why it is often called the system's state-dynamic matrix.

The stability of the system can be analyzed using this approach. If all eigenvalues (i.e. poles) have negative real parts, then it implies that the system is asymptotically stable. Also, damping factors associated with these

negative real eigenvalues are 1.0, which represents an exponentially decaying response. However, a damping factor less than 1.0 represents an oscillatory response of the system. In contrast, positive real part eigenvalues represent system instability.

The methods presented in this section are not the only method used, but they are the most common in the field of studying the stability of matrix converters. The transfer function approach is employed in particular to study the effect of each input and its effect on each output in a multiple-input multiple-output (MIMO) system. For instance, considering a frequency response of an arbitrary transfer function like the one shown in Figure7, if any input disturbance with frequency of $2.84\,rad/sec$, then this signal will be amplified by a scale of $12.6\,dB$, as it represents the natural frequency of this system. However, for disturbance with frequency of 15 rad/sec and above the effect of this signal will be attenuated naturally by system itself. Hence, the spectrum of frequencies that affect the system can be identified.

From this knowledge more appropriate controllers and/or filters can be designed for different types of disturbances **[11], [12], [20]–[22], [24], [25], [27].**

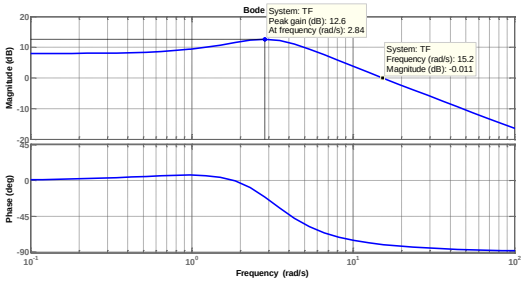

Figure. 7 Frequency response of an arbitrary function

5. Case Study: Modelling and Analysis of Matrix Converter Drive

It will use Matrix converter drives to control the induction motors However, the high starting current (several times as large as the rated current) is the most significant problem related to this type of machines. Matrix converter drives are capable of providing input and output sinusoidal waveforms with minimal distortion at adjustable input power factor. In addition, it permits this without bulky DC link energy storage devices, which makes it smaller and more compact. This helps to build small and compact drives. One example is to design a built-in drive which is fit inside the motor case. This considered as preferred design to be used in aerospace or military applications.

However, matrix converters have stability problems, which are affected by; maximum output power allowed, input voltage measurement, input filter, input current and voltage distortion, duty cycle calculation and filter time constant.

This section will explore a general steady state analysis of the whole matrix converter drive system feeding and induction motor in $d-q$ reference frames, provided that the operation is under constant $Volt/Hertz$ to keep constant flux in the machine. This will be done using a state space model, in which the stability of the system will be analyzed.

5.1 Dynamic State Space Modelling

The system presented in this section has a modification to the one presented in by adding another state, which is the motor speed. The system diagram shown in Figure 8 involves of a three-phase power supply fed an input filter then to an induction motor through the matrix converter, additionally, it is equipped with a digital low pass filter to provide clear reference voltage for switching the devices. These voltages are taken from capacitor voltage i.e. after input filter, and then transformed to $d-q$ reference frames, then back to three-phase frame again to produce modulation signals. Small signal analysis is carried out to determine the stability of the modelled system under constant volt per hertz, which to insure constant flux in the machine **[14], [16].**

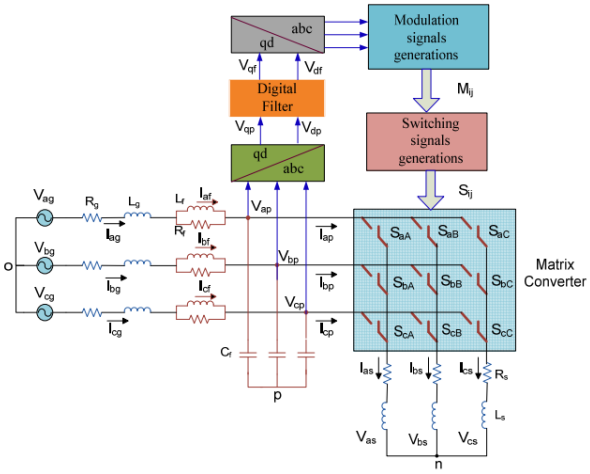

Figure .8 Schematic showing matrix converter drive system

Firstly the input voltage equations transferred to synchronous reference frame are presented as follows:

$$V_{dg} = R_g I_{dg} + L_g \frac{d}{dt} I_{dg} + \omega_p L_g I_{qg} + R_f\left(I_{dg} - I_{df}\right) + V_{dp} \quad (d-axis) \tag{23}$$

$$V_{qg} = R_g I_{qg} + L_g \frac{d}{dt} I_{qg} - \omega_p L_g I_{dg} + R_f\left(I_{qg} - I_{qf}\right) + V_{qp} \quad (q-axis) \tag{24}$$

Where: V_{dqg} – source voltage $d-q$ axis frames.

V_{dqp} – input capacitor voltage $d-q$ axis frames.

I_{dg} – input current dq axis frames.

ω_p – frequency of the supply.

Induction motor stator dynamic equation in $d-q$ axis can be presented as:

$$V_{ds} = R_s I_{ds} + \frac{d}{dt}\varphi_{ds} - \omega_s \varphi_{qs} \quad d-axis \tag{25}$$

$$V_{qs} = R_s I_{qs} + \frac{d}{dt}\varphi_{qs} + \omega_s \varphi_{ds} \quad q-axis \tag{26}$$

Induction motor rotor equations are presented as follows, provided that the rotor is squirrel cage type and it is short circuited i.e. zero voltage, hence:

$$0 = R_r I_{dr} + \frac{d}{dt}\varphi_{dr} - (\omega_s - \omega_r)\varphi_{qr} \quad d-axis \tag{27}$$

$$0 = R_r I_{qr} + \frac{d}{dt}\varphi_{qr} - (\omega_s - \omega_r)\varphi_{dr} \quad q-axis \tag{28}$$

Where: I_{dqs} – stator currents in dq axis frames.
I_{dqr} – rotor currents in dq axis frames.
V_{dqs} – stator voltages in dq axis frames.
R_s – stator resistance.
R_r – rotor resistance.
ω_r – rotor frequency.
φ_{dqs} – stator fluxes in dq frames.
φ_{dqr} – rotor fluxes in dq frames.

Stator and rotor linkage fluxes are presented as:

$$\varphi_{ds} = L_s I_{ds} + L_m I_{dr} \quad d-axis \tag{29}$$
$$\varphi_{qs} = L_s I_{qs} + L_m I_{qr} \quad q-axis \tag{30}$$
$$\varphi_{dr} = L_r I_{dr} + L_m I_{ds} \quad d-axis \tag{31}$$
$$\varphi_{qr} = L_r I_{qr} + L_m I_{qs} \quad q-axis \tag{32}$$

Where: L_m – the mutual inductance between rotor and stator.

Input filter capacitor voltage dynamic equations can be presented as follows:

$$C_f \frac{d}{dt} V_{abcp} = I_{abcg} - I_{abcp} \tag{33}$$

Where: V_{abcp} – input capacitor voltages.
I_{abcp} – input currents of matrix converter.
I_{abcg} – input supply currents.

Output and input currents and voltages are related as shown below:

$$V_{abcs} = [S_{abc}]\, V_{abcp} \tag{34}$$
$$I_{abcp} = [S_{abc}]^T\, I_{abcs} \tag{35}$$

Where: $[S_{abc}]$ is switching signal matrix.

$$V_{abcs} = [V_{as} \quad V_{bs} \quad V_{cs}]^T \qquad V_{abcp} = [V_{ap} \quad V_{bp} \quad V_{cp}]^T$$
$$I_{abcs} = [V_{as} \quad V_{bs} \quad V_{cs}]^T \qquad I_{abcp} = [I_{ap} \quad I_{bp} \quad I_{cp}]^T$$

The dynamic equation of damping resistor of the input filter is presented as follows:

$$L_f \frac{d}{dt} I_{df} + \omega_p L_g I_{qf} = R_f (I_{dg} - I_{df}) \quad d-axis \tag{36}$$

$$L_f \frac{d}{dt} I_{qf} + \omega_p L_g I_{df} = R_f (I_{qg} - I_{qf}) \quad q-axis \tag{37}$$

and likewise dynamic equations of input filter capacitor can be presented as follows:

$$C_f \frac{d}{dt} V_{dp} + \omega_p C_f V_{qp} = I_{dg} - I_{dp} \quad d-axis \tag{38}$$

$$C_f \frac{d}{dt} V_{qp} + \omega_p C_f V_{dp} = I_{qg} - I_{qp} \quad q-axis \tag{39}$$

Since the digital filter does not present phase angle difference to input voltage components, then they are given in $d-q$ reference frames, and by substituting currents using mapping between input and output currents in terms of the modulation matrix components. Hence:

$$\frac{d}{dt} V_{df} = \frac{1}{\tau}(V_{dp} - V_{df}) \tag{40}$$

$$\frac{d}{dt} V_{qf} = \frac{1}{\tau}(V_{qp} - V_{qf}) \tag{41}$$

Where: V_{df} – d axis of filter capacitor voltage.
V_{qf} – q axis of filter capacitor voltage.
τ – input filter time constant.

Dynamic equation that represents the developed electromagnetic torque in the machine is:

$$T_e = \frac{3}{2}\left(\frac{P}{2}\right)(\varphi_{ds} I_{qs} - \varphi_{qs} I_{ds}) \tag{42}$$

$$T_e = \frac{3}{2}\left(\frac{P}{2}\right)\frac{L_m^2}{L_r}\, I_{ds} I_{qs} \tag{43}$$

Rotor speed is presented as:

$$\frac{d}{dt}\omega_r = \frac{P}{2J}(T_e - T_{Load}) \tag{44}$$

Where: J – represent the moment of inertia of the machine.
T_{Load} – load torque.
T_e – electromagnetic torque.
P – number of poles.

Machine mechanical equation is given by:

$$\frac{d}{dt}\omega_r = \frac{T_e - T_{Load}}{J} - B\omega_r \tag{45}$$

Hence, the previously described dynamic equations can be rearranged using small signal analysis and using state space forms shown earlier, noting that it should be linearized around an operating point so that:

$$\frac{d}{dt} X = AX + BU \tag{46}$$
$$X = \Delta X + X_0 \tag{47}$$
$$U = \Delta U + U_0 \tag{48}$$

Where the states are chosen to be as:

$$X = [I_{qg}\ I_{dg}\ I_{qf}\ I_{df}\ V_{qp}\ V_{dp}\ V_{qf}\ V_{df}\ \varphi_{qs}\ \varphi_{ds}\ \varphi_{qr}\ \varphi_{dr}]^T$$

The input states are chosen to be the modulation signals, which can be presented as input stator voltages in dq reference frames, as the operating conditions have been obtained for specified stator voltages. These modulation signals depend on the input capacitor voltage and the output generated voltage. Thus, input states are chosen to be as:

$$U = [M_{qq}\ M_{qd}\ M_{dq}\ M_{dd}\ T_L]^T$$

Where:

$$M_{qq} = \frac{V_{qs} V_{qf}}{V_{qf}^2 + V_{df}^2} \tag{49}$$

$$M_{qd} = \frac{V_{qs} V_{df}}{V_{qf}^2 + V_{df}^2} \tag{50}$$

$$M_{dq} = \frac{V_{ds} V_{qf}}{V_{qf}^2 + V_{df}^2} \tag{51}$$

$$M_{dd} = \frac{V_{ds} V_{df}}{V_{qf}^2 + V_{df}^2} \tag{52}$$

and T_L – is the disturbance load torque.

The output states are selected to be:

$$Y = [I_{qg}\ I_{dg}\ V_{qp}\ V_{dp}\ I_{qs}\ I_{ds}\ \omega]^T$$

Hence, matrices A and B can be arranged as follows:

6. Simulation Results

Complex systems like the one presented in this paper has many outputs and they are affected by different inputs. Therefore, the method presented here facilitates the analysis of multiple-input multiple-output system. This is done by generating a matrix of transfer functions, in which relates each input state to each output state. And hence, the system can be treated as a single-input single-output system in terms of analysis approaches. Accordingly, more suitable design of controllers and filters can be constructed.

Different analysis approaches will be demonstrated in this section. The induction motor parameters are selected as shown in Table 1. While the source, and input filter, parameters are shown in Table 2.

Table 1 Induction motor parameters

Parameter	Value	Parameter	Value
Power	30 kw	V_s	400 volts
Poles	4	Cast-iron	frame 200L
L_m	33.633 mH	L_{ls}	1.674 mH
R_s	0.1313 Ω	L_{lr}	1.116 mH
f_s	50 Hz	R_r	0.06872 Ω
J	0.31 Kg.m^2	Type	squirrel cage IM

Table 2 Source and filter parameters

Parameter	Value
V_g	400 volt
R_g	0.01 Ohm
L_g	1 mH
L_f	225 mH
R_f	10 Ohm
C_f	27 µF

6.1 Transfer Function analysis and Frequency Response

Computer simulation results have been obtained using Matlab (2014) platform. Transfer function analysis was carried out in this section, which is done using the method explained in section 3. The state space model has been coded, and then the state space matrix was converted to a matrix that contains transfer functions. This can be achieved using "tf" command in Matlab. Additionally, Bode approach offers investigating the effect of closed-loop response of an input on associated output, from the knowledge of their open-loop transfer function. Therefore, bode plot i.e. frequency response of the transfer functions obtained was used to analyse the behaviour of each transfer function. Frequency response was obtained using "bode" command in Matlab. In this the relationship between each individual input and each individual output can be analysed and studied.

Figure 9 shows the bode plots of the system transfer functions for each input and output. For example, an input can be chosen and its effect on the output can be analyzed throughout the whole frequency spectrum. Considering input one in the model with output one can illustrate the effect of the voltage modulation index (M_{qq}) on the q-axis frame of the input current (I_{qg}), which is taken as an output here, this is to see the effect of changing the voltage transfer ratio on the input current, this can be demonstrated in Figure 10.

It shows steady DC gain of $(40\,dB)$ and (0 degree) phase, then the gain reaches $(64\,dB)$ at frequency of $(811\,Hz)$ while the phase drops to $(-45\,degrees)$. Then the gain drops to $(41\,dB)$ when the phase is (-139 degrees) (pole action). After that, the gain starts to rise again to its peak of $(69.4\,dB)$ at frequency $(942\,Hz)$ (zero action), and this defines the natural frequency of the system. It is worth to note that any disturbances at this frequency will be amplified and drive the system to unstable operation. The point of zero gain defines the crossover frequency which occurs at $(9.35\,kHz)$, this frequency is critical since the errors at this gain crossover are destructive. Gain margin is infinity as the bode plot never crossed (-180 degrees), hence there is no phase crossover frequency, therefore the gain margin cannot be determined, this implies that the system is inherently stable, and the phase margin is (5.78 degrees), which is too low to have well damped stable system, however, the closed loop system is stable as the gain margin is infinite. Furthermore, as it is known, the bode plot approach gives the closed loop response of the system from the knowledge of the open loop transfer function, so by examining the system response for a unity feedback using a step input signal, the system behaviour can be shown as illustrated in Figure 11. It can be noticed that the system has oscillation at starting but then it reaches steady state after two milliseconds.

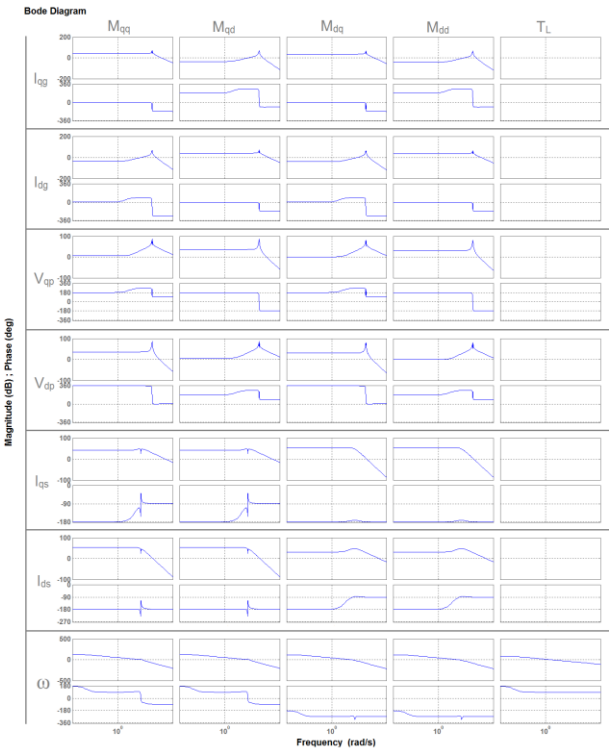

Figure. 9 Frequency response relating inputs to outputs

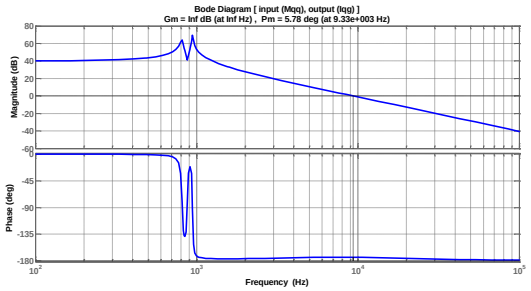

Figure .10 Frequency response for transfer function relating input (Mqq) and output (Iqp)

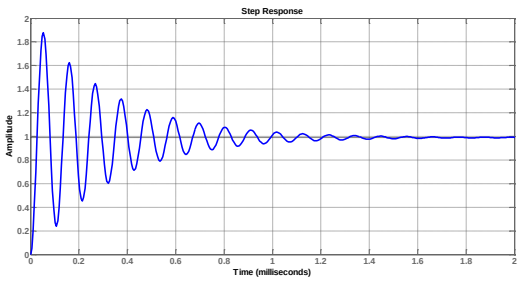

Figure .11 Step response for transfer function relating input (M_{qq}) and output (I_{qp})

Considering another example, the transfer function illustrating the relationship between input (M_{qd}) with the $q-axis$ component of the load current (I_{qs}), which is shown in Figure 12. The gain margin of the system is ($-41.4\ dB$) at (0 Hz) frequency, and the phase margin is (90 degrees) at frequency of ($24.6\ kHz$), which defines that any disturbance above this frequency will be attenuated. Moreover, it defines that the transfer function of this relation is stable. In addition, it can be seen from the step response of the unity feedback closed loop transfer function shown in Figure 13, which can be seen that the system has fast stable response. However, it is worth to state that this transfer function has two peak points with high gain at low frequency (around the system frequency "50 Hz"), this leads the system to be prone to stability operation, as those frequencies might be needed for normal operation (i.e different speed or load torque demands).

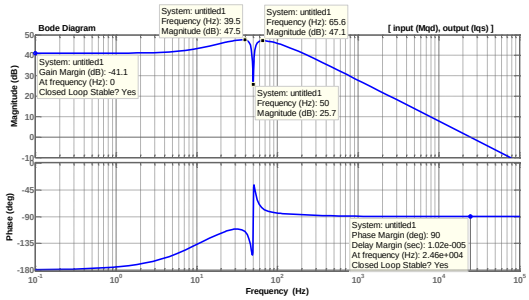

Figure. 12 Frequency response for transfer function relating input (M_{qd}) and output (I_{qs})

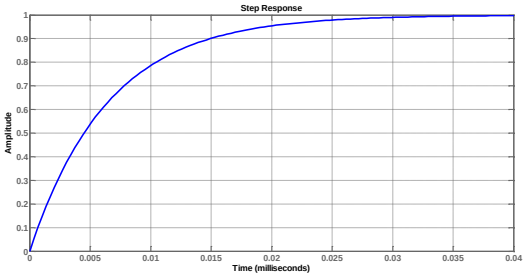

Figure. 13 Step response for transfer function relating input (M_{qd}) and output (I_{qs})

6.2 Pole-Zero Map Analysis

Similar to the frequency response analysis, pole-zero map tools for the same transfer functions was obtained. Since the input filter resistance is vital part in input filter, it was decided to analyse the effect of changing the value of damping resistance and monitor its effect on the stability using the pole-zero map analyses, which is based on the root locus of each transfer function in the system. Using the m-file. The pole-zero maps using "iopzmap" command in Matlab were obtained for different values of damping resistor (from $0-100\ Ohm$). The results are as shown in Figure 14.

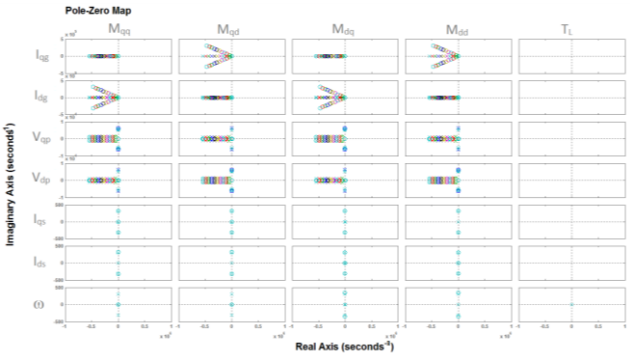

Figure 14: Pole-zero maps of the whole system transfer functions for different values of Rf

It can be noticed that changing the damping resistance value only affect the inputs (I_{qg}, I_{dg}, V_{qp} and V_{dp}), the system stability increases as the resistance increases, but on the expense of the efficiency. This can be illustrated in Figure 15, considering the transfer function relating the input (M_{qd}) with the output (I_{qg}), the poles and zeros of the system are moving toward the negative part of the root locus, i.e. more stable system as the resistance increases.

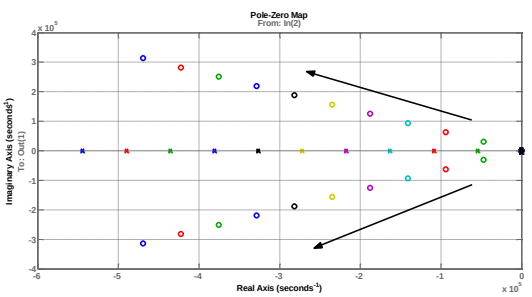

Figure. 15 Pole-zero map of the transfer function relating input (M_{qd}) and output (I_{qg})

Moreover, changing the values of other input filter components like (Cf and Lf) has been considered, and the pole-zero maps have been obtained. The results regarding the filter inductance were obtained, and it has been found that the changing this value does not have significant effect on the poles and zeros positions for each transfer functions, this can be seen in Figure 16.

The value of the filter capacitor Cf has been changed (from 1µF up to 500µF), and it has been noticed that this value has more effect on changing the poles and zeros position, yet, it is low effect compared to the variation made by changing the value of the damping resistor, which can be seen in Figure 17. Therefore, it can be concluded that damping resistor has the major effect on the system regarding system stability.

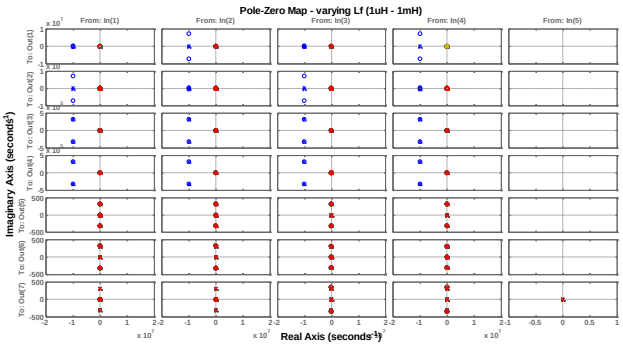

Figure. 16 Pole-zero maps of the whole system transfer functions for different values of Lf.

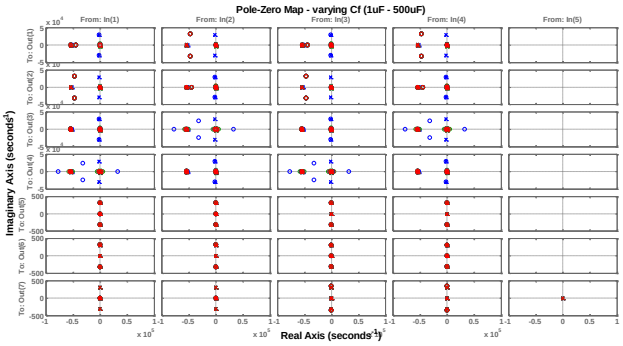

Figure .17 Pole-zero maps of the whole system transfer functions for different values of Cf.

6.3 Eigenvalues Analysis Results

The stability of the system has been examined by determining the eigenvalues of the matrix (A). The eigenvalues that has negative real part are stable, and the more positive the more stable the system . On the other hand, the positive real eigenvalues represent unstable system. The system eigenvalues are obtained using Matlab and it can be seen in Figure 18, which shows the dominant eigenvalues (i.e. the ones close to the positive real part of the plane) which have dominant effect on the stability of a system. It can be noticed that the system has an unstable eigenvalue at (+268), which defines the system as unstable. Therefore, different system parameters have been changed and tested in order to manipulate the unstable eigenvalue.

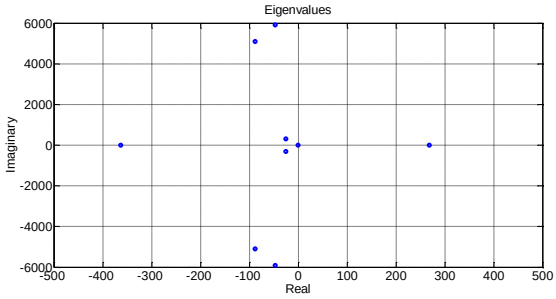

Figure .18 Dominant Eigenvalues of matrix A

Firstly, the value of filter capacitor has been changed (from 1µF up to 500 µF) to see its effect on eigenvalues. It has been concluded that unstable eigenvalue remains unchanged i.e. the filter capacitor does not alter this value. However, other dominant eigenvalues have been changed, and simulation results show that increasing the filter capacitor force the eigenvalues to move towards the unstable region (positive real part), this is illustrated in Figure 19.

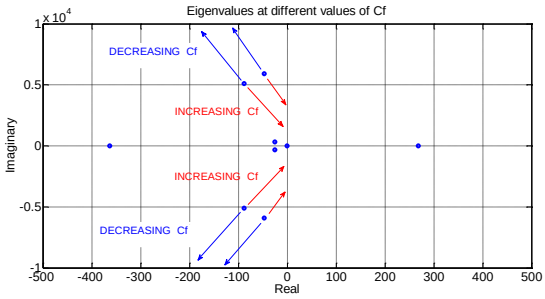

Figure. 19 Dominant Eigenvalues of matrix A with different values of Cf

The value of the filter inductance has also been changed to try shifting the unstable eigenvalue. The value of filter inductance Lf has been varied from (1µH up to 1mH), and it can be concluded that increasing the value of Lf does not alter the unstable eigenvalue. However, it forces dominant eigenvalues to move towards the stable region i.e. the negative real part as shown in Figure 20.

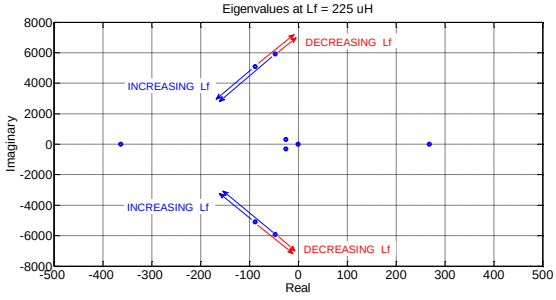

Figure .20 Dominant Eigenvalues of matrix A with different values of Lf

Changing the value of the digital filter time constant is another attempt to shift the unstable eigenvalue. This value has been changed from (1µsec up to 100msec), and consequently the unstable value did not change, instead

two eigenvalues were moving towards the positive real part of the plane as the value of time constant increased, which can be seen in Figure 21.

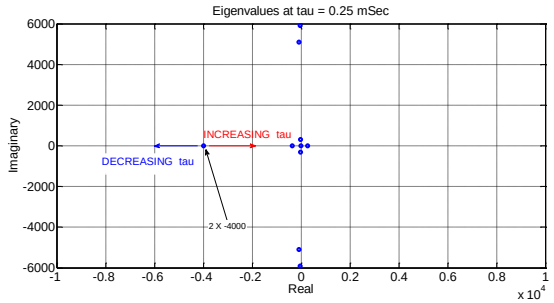

Figure. 21 Dominant Eigenvalues of matrix A with different values of digital filter time constant

7. Discussion

Matrix converter system with an input filter, low pass digital filter, and an induction motor has been modelled and analysed using small signal analysis. Then, it was linearized about an operating point, before modelling it as a state space model. State variables are selected in a way that examine the effect of voltage modulation indices and the load disturbance torque on the input current, input voltages and stator voltages and currents all in d-q reference frames. Using Matlab platform, the system was analysed, this was done through converting the state space model into a set of transfer functions relating each state input to each state output. This way offers the ability of studying the effect that each input has on every output separately. This is advantageous, because a complicated system that has multiple-inputs and multiple-outputs can be studied and analysed as simple as a single input-single single-output system, which can be done by means of classic control theories.

Bode approach offers the ability of analysing the effect of closed-loop response of an input on associated output, from the knowledge of their open-loop transfer function. Therefore, bode plot i.e. frequency response of the transfer functions obtained was used to analyse the behaviour of each transfer function. Also, this was confirmed using step response for the same transfer function. Moreover, it is worth to mention that some of the transfer functions have stable operation throughout the whole frequency spectrum and have the ability to reject any disturbances. However, some other have fragile stability condition which might drive the system unstable if the operation condition is changed, or if a certain disturbance presented. Others have totally unstable response thought the frequency spectrum, and it was concluded that motor parameters have major effect on the stability. This is particularly stands for the motor type and parameters used for this model, it might not be the case for each system, besides the focus was on the method of extracting transfer function more than exploring solutions for system instability.

Furthermore, it has been concluded that this instability might be related to this system only with its specific parameters, and/or the operating point used to derive the model. Therefore, different system parameters were changed to modify the unstable poles and zeros. This was tested using the migration of the eigenvalues of matrix (A). For example, the damping resistance has the major effect on the stability of the system. Choosing a low value of the damping resistor Rf gives significant improvement of filtering the high frequency components, but on the expense of lowering the efficiency of the system. Input filter inductor Lf and capacitor Cf were varied separately in order to shift the unstable eigenvalue, yet the effect was very small. These results were proven using the pole-zero maps for each transfer function and it led to the same results. Furthermore, the induction motor parameters were altered to see their effect on the unstable margin, and it has been concluded that rotor and stator resistance have significant influence on the unstable eigenvalue, also, the magnetising inductance of the rotor has the same effect on altering the unstable eigenvalue. Yet, manipulating these parameters is beyond the scope of this project.

Additionally, the selection of state variables, inputs and outputs of the state space model was not unique, it could be rearranged to relate different input and output states. For instance this has been examined by selecting the output states to be as same as the state variables, the outcome of this would be matrix including transfer functions relating same number of input to more outputs (in this case 13 state outputs as there is 13 state variables), This can be seen in Figure **22**.

Moreover, different state variables can be selected to study the effect of other parameters, for example, the effect of rotor resistance or magnetising inductance could be examined, which has been noted that they significantly affect the stability of the system.

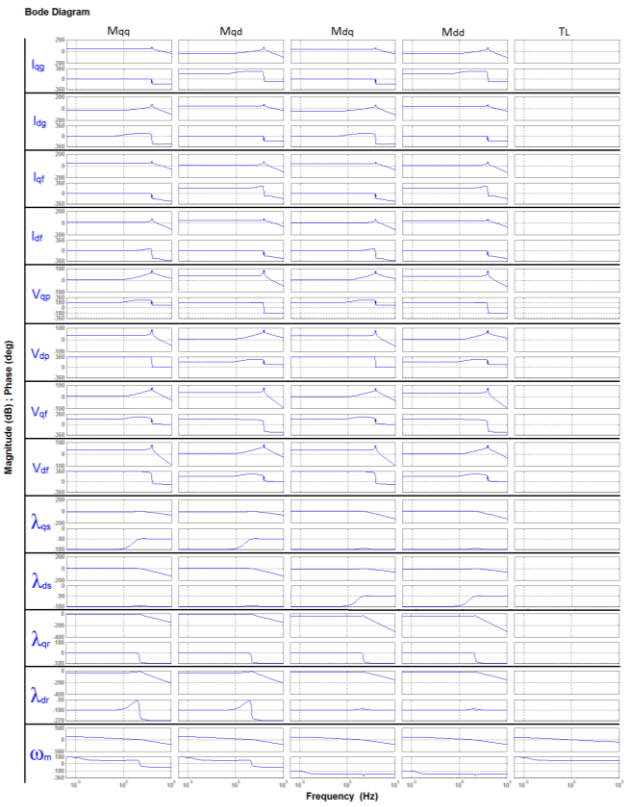

Figure. 22 Bode plots for transfer functions relating state variables to inputs

Conclusions

State space model of an AC/AC matrix converter system drive feeding induction motor was employed to analyse the stability of the system. In this paper steady state model was derived and tested in Matlab (2014) platform. Also, a new method of analysing the system stability was presented, which makes the MIMO system possible to be analysed as simple as a SISO system. Using various stability methods, like transfer function analysis and eigenvalue analysis, which were exploited to examine the stability of the system. Using the transfer function approach, the system was examined for different cases of inputs and outputs, and thereby, this provides a tool to design more appropriate controllers and filters for the system. Also, this method was tested with different numbers of inputs and outputs, which add more credits to it. In eigenvalue analysis, it was noticed that the stability is significantly affected by the system parameters. Filter parameters have huge impact on the stability, and simulation results show that filter damping resistor has the major effect. Furthermore, motor parameters change as the temperature changes, and hence the stability of the system can be affected. Therefore, a model that includes equations that can describe this change will be a worthy start point for future studies.

References

[1] Z. Malekjamshidi, M. Jafari, D. Xiao, and J. Zhu, "Analysis of direct matrix converter operation under various switching patterns," *Proc. Int. Conf. Power Electron. Drive Syst.* 2015-Augus, June,. 630, 2015.

[2] E. Purwanto, F. D. Murdianto, D. Wahyu Herlambang, G. Basuki, and M. P. Jati, "Three-phase direct matrix converter with space vector modulation for induction motor drive," *Proc. ICAITI 2019 - 2nd Int. Conf. Appl. Inf. Technol. Innov. Explor. Futur. Technol. Appl. Inf. Technol. Innov.*. 11, 2019.

[3] P. W. Wheeler, J. Rodríguez, J. C. Clare, L. Empringham, and A. Weinstein, "Matrix converters: A technology review," *IEEE Trans. Ind. Electron.,*. 49, 2. 276, 2002.

[4] M. A. Perez, C. A. Rojas, J. Rodriguez, and H. Abu-Rub, "A simple modulation scheme for a three-phase direct matrix converter," *IEEE Int. Symp. Ind. Electron.,*. July 2015, 105, 2012.

[5] S. H. Hosseini and E. Babaei, "A new generalized direct matrix converter," *IEEE Int. Symp. Ind. Electron.,*. 2,. 1071, 2001.

[6] H. Karaca and R. Akkaya, "An approach for controlling of matrix converter in input voltage variations," *Eng. Lett.,*. 17,. 2, 2009.

[7] R. Ghoni, A. N. Abdalla, S. P. Koh, H. F. Rashag, and R. Razali, "Issues of matrix converters: Technical review," *Int. J. Phys. Sci.*, 6.,15, 3628, 2011.

[8] S. Orcioni, G. Biagetti, P. Crippa, and L. Falaschetti, "A driving technique for AC-ac direct matrix converters based on sigma-delta modulation," *Energies,*. 12,. 6,. 1, 2019.

[9] H. Karaca, "Control of Venturini Method Based Matrix Converter in Input Voltage Variations," *Proc. Int. MultiConference Eng. Comput. Sci. 2009*, II, 1, 1412, 2009.[Online]. Available: http://www.iaeng.org/publication/IMECS2009/

[10] R. W. Erickson, *Converter Circuits*. 1997.

[11] J. Rodriguez, M. Rivera, J. W. Kolar, and P. W. Wheeler, "A review of control and modulation methods for matrix converters," *IEEE Trans. Ind. Electron.,*. 59,. 1. 58, 2012.

[12] K. . Kandaswamy and M. . Sharmila, "Industrial Drive Performance Analysis with Direct Matrix Converter," *Open Acad. J. Adv. Sci. Technol.*, 1,. 1, 6, 2017.

[13] Y. Han, B. Han, X. Ni, P. Qiu, and Z. Xiang, "Research on grounding mode of AC-AC converter system,". 13026, 2022.

[14] K. Govindarajan and D. Anbazhagan, "Direct Space Vector Modulated Matrix Converter and its Dynamic Model Study," no. May 2012, 2016.

[15] K. Omrani, M. A. Dami, and M. Jemli, "A SVM control strategy for a direct matrix converter," *Int. Conf. Green Energy Convers. Syst. GECS 2017*, 3, 2017.

[16] M. Mihret, "Modeling, stability analysis and control of a direct AC/AC matrix converter based systems," 2012.

[17] L. Ming *et al.*, "A SiC-Si Hybrid Module for Direct Matrix Converter With Mitigated Current Spikes," *IEEE J. Emerg. Sel. Top. Power Electron.,*. 10,. 4,. 3805, 2022.

[18] P. Kiatsookkanatorn and S. Sangwongwanich, "A Unified PWM Strategy to Reduce Minimum Switching Number for Matrix Converters," *2022 Int. Power Electron. Conf. IPEC-Himeji 2022-ECCE Asia*2, 83, 2022.

[19] A. Dasgupta and P. Sensarma, "An integrated filter and controller design for direct matrix converter," *IEEE Energy Convers. Congr. Expo. Energy Convers. Innov. a Clean Energy Futur. ECCE 2011, Proc.*, no. May 2014,. 814, 2011.

[20] J. Igney and I. Hahn, "Modulation Strategy and Control Range Function for Matrix Converters Without Trigonometric Functions," *2022 Int. Symp. Power Electron. Electr. Drives, Autom. Motion, SPEEDAM 2022*,. 553, 2022.

[21] P. Patel and M. A. Mulla, "Space vector modulated three-phase to three-phase direct matrix converter," *EEEIC 2016 - Int. Conf. Environ. Electr. Eng.*, no. Imc, 2016.

[22] A. K. Singh and A. K. Singh, "Implementation of Direct Matrix Converter using hybrid modulation with minimized losses," *IECON Proc. (Industrial Electron. Conf.*, 2, 846, 2013.

[23] A. Babaei and W. Ziomek, "The Improvement of Power Quality in an ac-ac Direct Matrix Converter by Using Hybrid Filters," no. July,. 20, 2022.

[24] P. Resutik, S. Kascak, and J. Kellner, "Design, Simulation, and Analysis of Compact 3x1 Matrix

Module Prototype in 3x3 Matrix Converter Application," *14th Int. Conf. ELEKTRO, ELEKTRO 2022 - Proc.*, 2022.

[25] J. M. Lozano-Garcia and J. M. Ramirez, "Voltage compensator based on a direct matrix converter without energy storage," *IET Power Electron.*, 8, 3,. 321, 2015.

[26] A. El Aroudi, E. Rodriguez, and M. Orabi, "Modeling of switching frequency instabilities in buck- based DC – AC H-bridge inverters," *Int. J. Circuit Theory Appl.*, no. March 2015,. 213, 2010.

[27] M. Leubner, N. Remus, M. Stübig, and W. Hofmann, "Active stabilization of direct matrix converter input side filter through grid current control," *Conf. Proc. - IEEE Appl. Power Electron. Conf. Expo. - APEC*, 2016-May, 2,. 2175, 2016.

[28] C. Gili, G. D. Lozano, A. Péres, and S. V. G. Oliveira, "Experimental study of a direct matrix converter driving an induction machine," *COBEP 2011 - 11th Brazilian Power Electron. Conf.*,. 232, 2011.

[29] A. Dasgupta and P. Sensarma, "Filter design of direct matrix converter for synchronous applications," *IEEE Trans. Ind. Electron.*, 61, 12,. 6483, 2014.

[30] S. Ansari and A. Chandel, "Simulation based comprehensive analysis of direct and indirect matrix converter fed asynchronous motor drive," *2017 4th IEEE Uttar Pradesh Sect. Int. Conf. Electr. Comput. Electron. UPCON 2017*, 2018-Janua, 9, 2017.

[31] Z. Malekjamshidi, M. Jafari, and J. Zhu, "Analysis and comparison of direct matrix converters controlled by space vector and Venturini modulations," *Proc. Int. Conf. Power Electron. Drive Syst.*,. 2015-Augus,. July,. 635, 2015.

[32] L. R. Merchan, J. M. L. Garcia, A. Pizano-Martinez, E. A. Zamora-Cardenas, H. J. Estrada-Garcia, and L. C. Razo-Vargas, "Output filter control for matrix converter in synchronous applications," *2016 IEEE Int. Autumn Meet. Power, Electron. Comput. ROPEC 2016*, November, 2017.